Journal of Controlled Release 291 (2018) 135–146

Contents lists available at ScienceDirect

Journal of Controlled Release

journal homepage: www.elsevier.com/locate/jconrel

Anionic 1,2-distearoyl-sn-glycero-3-phosphoglycerol (DSPG) liposomes induce antigen-specific regulatory T cells and prevent atherosclerosis in mice

Naomi Benne[a], Janine van Duijn[a], Fernando Lozano Vigario[a], Romain J.T. Leboux[a], Peter van Veelen[b], Johan Kuiper[a], Wim Jiskoot[a], Bram Slütter[a,*]

[a] Divison of BioTherapeutics, Leiden Academic Center for Drug Research, Leiden, The Netherlands
[b] Center for Proteomics and Metabolomics, Leiden University Medical Center, Leiden, The Netherlands

ARTICLE INFO

Keywords:
Liposomes
Tolerance
Atherosclerosis
Regulatory T cells
C1q
Vaccination

ABSTRACT

Atherosclerosis is the predominant underlying pathology of many types of cardiovascular disease and is one of the leading causes of death worldwide. It is characterized by the retention of oxidized low-density lipoprotein (ox-LDL) in lipid-rich macrophages (foam cells) in the intima of arteries. Autoantigens derived from oxLDL can be used to vaccinate against atherosclerosis. However, a major challenge is the induction of antigen-specific Tregs in a safe and effective way. Here we report that liposomes containing the anionic phospholipid 1,2-distearoyl-sn-glycero-3-phosphoglycerol (DSPG) induce Tregs that are specific for the liposomes' cargo. Mechanistically, we show a crucial role for the protein corona that forms on the liposomes in the circulation, as uptake of DSPG-liposomes by antigen-presenting cells is mediated *via* complement component 1q (C1q) and scavenger receptors (SRs). Vaccination of atherosclerotic mice on a western-type diet with DSPG-liposomes encapsulating an LDL-derived peptide antigen significantly reduced plaque formation by 50% and stabilized the plaques, and reduced serum cholesterol concentrations. These results indicate that DSPG-liposomes have potential as a delivery system in vaccination against atherosclerosis.

1. Introduction

Atherosclerosis is a disease involving large and medium-sized arteries, which affects millions of people worldwide [1]. It is initiated by the retention of LDL in the subendothelial space of arteries, and subsequent oxidation and uptake of LDL (oxLDL) by infiltrating macrophages leading to foam cell formation [2]. In recent years, it has become clear that atherosclerosis is a chronic inflammatory disease. Cells of both the innate and adaptive immune system, such as macrophages, dendritic cells (DCs), T and B lymphocytes, are present in atherosclerotic plaques and are involved in the progression of the disease [3,4]. While there is still debate about the specific role of certain cell types in atherosclerosis, the general consensus is that T helper 1 (Th1) $CD4^+$ T cells are pro-atherogenic, while regulatory T and B cells (Tregs and Bregs, respectively) are protective [5,6]. Tregs are known to be vital for immune suppression, regulation, and resolution of

Abbreviations: ACK, Ammonium-Chloride-Potassium; AEC, 3-amino-9-ethylcarbazole; BCIP, 5-bromo-4-chloro-3-indolyl phosphate; BMDC, Bone marrow-derived dendritic cell; Breg, Regulatory B cell; BSA, Bovine serum albumin; C1q, Complement component 1q; CFA, Complete Freund's adjuvant; DC, Dendritic cell; DLS, Dynamic light scattering; DPPE-Rho, 1,2-dipalmitoyl-sn-glycero-3-phosphoethanolamine-N-(lissamine rhodamine B sulfonyl); DPPS, 1,2-dipalmitoyl-sn-glycero-3-phospho-L-serine; DPTAP, 1,2-dipalmitoyl-3-trimethylammonium-propane; DSPC, 1,2-distearoyl-sn-glycero-3-phosphocholine; DSPG, 1,2-distearoyl-sn-glycero-3-phosphoglycerol; EDTA, Ethylenediaminetetraacetic acid; FCS, Fetal calf serum; FOXP3, Forkhead box P3; FVIII, Factor VIII; GM-CSF, Granulocyte-macrophage colony-stimulating factor; HRP, Horseradish peroxidase; i.v., intravenously; IFA, Incomplete Freund's adjuvant; IFN, Interferon; IL, Interleukin; IMDM, Iscove's Modified Dulbecco's Medium; LDL, Low-density lipoprotein; LE, Loading efficiency; LPS, Lipopolysaccharide; MHC, Major histocompatibility complex; MOMA2, Macrophages/monocytes antibody; NBT, nitro blue tetrazolium; OCT, Optimal cutting temperature; PB, Phosphate buffer; PBS, phosphate-buffered saline; PDI, Polydispersity index; PG, Phosphatidylglycerol; PMA, phorbol 12-myristate 13-acetate; poly I, polyinosinic acid; PS, Phosphatidylserine; RPMI 1640, Roswell Park Memorial Institute Medium; SDS-PAGE, sodium dodecyl sulfate-polyacrylamide gel electrophoresis; SLE, Systemic lupus erythematosus; SR, Scavenger receptors; TFA, Trifluoroacetic acid; TGF-β, Transforming growth factor β; Th, T helper cell; TIM4, T-cell immunoglobulin- and mucin-domain-containing molecule 4; Treg, Regulatory T cell; WB, Western blotting; WT, Wild-type; WTD, Western-type diet; Z_{ave}, Z-average diameter

* Corresponding author at: Einsteinweg 55, 2333 CC Leiden, The Netherlands.
E-mail address: b.a.slutter@lacdr.leidenuniv.nl (B. Slütter).

https://doi.org/10.1016/j.jconrel.2018.10.028
Received 1 May 2018; Received in revised form 27 September 2018; Accepted 22 October 2018
Available online 23 October 2018

inflammation after infection [7]. They form a subset of $CD4^+$ T cells that express the transcription factor forkhead box P3 (FOXP3) and the IL-2 receptor α chain (CD25). Tregs mediate tolerance by the production of the anti-inflammatory cytokines interleukin (IL)-10 and transforming growth factor (TGF)-β [8], consuming IL-2, interrupting effector T cell metabolism or even lysing effector T cells [9]. In many inflammatorydiseases, including atherosclerosis [10–12], Tregs have a reduced function or ability to proliferate. Current strategies for treatment of such disorders involve systemic suppression of inflammation with drugs or by selective cell depletion. However, these therapies can result in severe side effects, especially upon long-term treatment [13–15]. A more specific strategy would be to design a vaccine that induces specific tolerance through induction of Tregs that recognize the autoantigens involved in inflammatory diseases. LDL has been identified as the most relevant antigen in atherosclerosis, as it is important in the initiation of atherosclerosis [2,16]. Indeed, oxLDL-specific T cells have been found in human atherosclerotic plaques [17], and antibodies against ApoB100 (the apolipoprotein of LDL) have been identified in patients with cardiovascular disease [18–20]. LDL, ApoB100, ApoB100-derived peptides and antibodies against ApoB100-derived peptides have successfully been used as vaccine targets in mice [21–28].

While these studies show a reduction in atherosclerotic plaque formation in mice, only a few have been designed with the goal of inducing antigen-specific Tregs [29] or using complex formulations [24]. To our knowledge, there are no reports about the use of athero-protective antigens with advanced drug delivery formulations. Immunotherapy with so-called tolerogenic DCs (DCs pulsed *ex vivo* with antigens and IL-10 or TGF-β) or oxLDL-pulsed (apoptotic) DCs have been successful at inducing Tregs. However, these treatments are expensive, as they require *ex vivo* isolation and long-term culturing of DCs under GMP conditions [30–32]. Moreover, there is evidence that DCs induced in this way can lose their migratory and T cell activation potential or can even revert to a pro-inflammatory phenotype *in vivo* [33]. Therefore, there is a need for vaccine formulations that induce tolerogenic DCs and ApoB100-specific Tregs *in vivo*.

Liposomes are established delivery vehicles which can deliver a drug or antigen directly into the cell [34]. Moreover, their properties and contents can be fine-tuned to the therapy. For instance, it has been shown that anionic liposomes composed of phosphatidylserine (PS) resemble apoptotic cells (PS becomes exposed on the surface of apoptotic cells [35]). Through SR-mediated uptake by antigen-presenting cells, PS-containing liposomes mediate an anti-inflammatory effect in diabetic and edema mouse models [36,37]. Furthermore, empty PS liposomes used in the treatment of atherosclerosis reduced plaque size and cellular content to a similar extent as injection of apoptotic cells [38]. In contrast, cationic liposomes are known to be pro-inflammatory, which is advantageous for vaccination against infectious diseases or the treatment of cancer [39,40].

Here we assessed whether we can use liposomal formulations to induce antigen-specific Tregs, and subsequently use these liposomes to encapsulate a newly identified ApoB100-derived peptide to provide protection against atherosclerosis. We report that phosphatidylglycerol (PG)-containing liposomes mediate a superior antigen-specific Treg response compared to the free antigen, PS liposomes or cationic liposomes. Moreover, we show that an SR-independent pathway for PG-containing liposomes mediates the induction of Tregs. Furthermore, we identified a major-histocompatibility complex (MHC)-II-restricted ApoB100-derived peptide using a peptidomics strategy, which, when encapsulated in DSPG liposomes, successfully reduced atherosclerotic plaque formation in an atherosclerosis mouse model.

2. Materials and methods

2.1. Materials

The lipids 1,2-distearoyl-sn-glycero-3-phosphocholine (DSPC), 1,2-distearoyl-sn-glycero-3-phosphoglycerol (DSPG), 1,2-dipalmitoyl-sn-glycero-3-phospho-L-serine (DPPS), 1,2-dipalmitoyl-3-trimethylammonium-propane (DPTAP), and 1,2-dipalmitoyl-sn-glycero-3-phosphoethanolamine-N-(lissamine rhodamine B sulfonyl) (DPPE-Rho) were obtained from Avanti Polar Lipids (Alabaster, AL, USA). Cholesterol was purchased from Sigma-Aldrich (Zwijndrecht, the Netherlands). The ovalbumin-derived peptide OVA323 (ISQAVHAAHAEINEAGR) was obtained from Invivogen (San Diego, California, USA). The ApoB100-derived peptide p3500 (LSQEYSGSVANEANV) was synthesized by GenScript (Piscataway, New Jersey, USA). Polycarbonate track-etched membranes with a pore size of 400 nm and 200 nm were obtained from Millipore (Kent, UK).

For cell culture, Ca^{2+}- and Mg^{2+}-free phosphate-buffered saline (PBS), Iscove's Modified Dulbecco's Medium (IMDM), Roswell Park Memorial Institute Medium (RPMI 1640), L-glutamine, and penicillin/streptomycin were purchased from Lonza (Basel, Switzerland). Lipopolysaccharide (LPS) extracted from *Salmonella Typhosa,* phorbol 12-myristate 13-acetate (PMA), ionomycin, brefeldin A, β-mercaptoethanol, and polyinosinic acid (poly I) were purchased from Sigma-Aldrich (Zwijndrecht, the Netherlands). Granulocyte-macrophage colony-stimulating factor (GM-CSF) was purchased from PeptroTech (London, UK). Human C1q was purchased from Abcam (Cambridge, UK). Fetal calf serum (FCS) was purchased from GE Healthcare (Little Chalfont, UK). Human C1q-depleted serum and normal human serum were a generous gift from Dr. F. A. Ossendorp (Department of Immunohematology and Blood Transfusion, Leiden University Medical Centre).

The antibodies CD4-PerCP (RM4–5), Ly-6G (1A8) and NK1.1 (PK136) were purchased from BD Biosciences (NJ, USA). CD4-APC (GK1.5), CD4-FITC (GK1.5) and Thy1.2-PerCP-Cy5.5 (53-2.1) were purchased from Biolegend (CA, USA). CD11b-eFluor450 (M1/70), CD25-FITC (PC61.5), CD45.1-eFluor450 (A20), CD45.1-PE (A20), Fixable viability dye-APC-eFluor780, Fixable viability dye-eFluor506, FOXP3-eFluor450 (FJK-16 s), IFNγ-PE (XMG1.2), IL-10-APC (JES5-16E3), IL-17A-PE (eBio17B7), IL-4-APC (11B11), Ki67-FITC (SolA15), Ly-6C-PerCP-Cy5.5 (HK1.4), Thy1.2-PE-Cy7 (53–2.1), and FOXP3/transcription factor staining kit were purchased from eBioscience (Thermofisher Scientific, MA, USA). CCR2-APC (#475301) was purchased from R&D systems (MN, USA).

For sodium dodecyl sulfate-polyacrylamide gel electrophoresis (SDS-PAGE) and Western blotting (WB), Laemmli sample buffer, Precision Plus Protein™ all blue prestained protein standards, Mini-PROTEAN® Tetra vertical electrophoresis cell, Mini Trans-Blot® cell, blot absorbent filter paper, and 4–20% Mini-PROTEAN® precast gels were purchased from Bio-Rad (Veenendaal, the Netherlands). Bovine serum albumin (BSA), Polysorbate 20, tris-glycine-SDS buffer 10× concentrate, tris(hydroxymethyl)aminomethane, glycine, and 3-amino-9-ethylcarbazole (AEC) staining kit were purchased from Sigma-Aldrich (Zwijndrecht, the Netherlands). Nitrocellulose membrane with a 0.45 μm pore size was obtained from GE Healthcare (Little Chalfont, UK). Mouse monoclonal biotinylated anti-C1q antibody (JL-1) was purchased from Abcam (Cambridge, UK). Streptavidin-horseradish peroxidase (HRP) was purchased from Thermofisher Scientific (MA, USA).

Optimal cutting temperature (OCT) formulation Tissue-Tek® was obtained from Sakura Finetek (CA, USA). For immunohistochemical staining, Hematoxylin, Oil-Red-O, Sirius Red, and anti-rat IgG (whole molecule)–alkaline phosphatase antibody produced in goat were purchased from Sigma-Aldrich (Zwijndrecht, the Netherlands), rat anti-mouse macrophages/monocytes antibody (MOMA2) was purchased from Bio-Rad (Veenendaal, the Netherlands). 5-bromo-4-chloro-3-indolyl phosphate (BCIP)/nitro blue tetrazolium (NBT) substrate system buffer was purchased from DAKO (Agilent, CA, USA).

2.2. Animals

C57BL/6, OT-II transgenic, T-cell immunoglobulin- and mucin-domain-containing molecule 4 (TIM4)$^{-/-}$ and LDLr$^{-/-}$ mice on a C57BL/6 background were purchased from Jackson Laboratory (CA, USA), bred in-house under standard laboratory conditions, and provided with food and water *ad libitum*. LDLr$^{-/-}$ mice were fed a Western-type diet (WTD) containing 0.25% cholesterol and 15% cocoa butter (Special Diet Services, Essex, UK). All animal work was performed in compliance with the Dutch government guidelines and the Directive 2010/63/EU of the European Parliament. Experiments were approved by the Ethics Committee for Animal Experiments of Leiden University.

2.3. Bone marrow-derived dendritic cells (BMDCs)

Bone marrow was isolated from the tibias and femurs of C57BL/6 or TIM4$^{-/-}$ mice. A single-cell suspension of bone marrow cells was obtained by using a 70-μm cell strainer (Greiner Bio-One B.V., Alphen aan den Rijn, NL). The cells were cultured in IMDM (Lonza) supplemented with 2 mM L-glutamine, 8% (*v*/v) FCS, 100 U/mL penicillin/streptomycin (Lonza), and 50 μM β-mercaptoethanol (Sigma) at 37 °C and 5% CO_2 in 95 mm Petri dishes (Greiner Bio-One B.V., Alphen aan den Rijn, NL) and 20 ng/mL GM-CSF (PeproTech) for 10 days. Medium was refreshed every other day.

2.4. Immunoprecipitation

BMDCs were incubated with 10% serum from LDLr$^{-/-}$ mice on a WTD activated with 0.1 μg/mL LPS. Affinity-purification of MHC-II (I-Ab) molecules from BMDCs and subsequent peptide elution was performed as described previously [41]. Approximately 50 × 10^6 BMDCs were lysed in 0.5 mL lysis buffer (50 mM Tris-Cl pH 8.0, 150 mM NaCl, 5 mM Ethylenediaminetetraacetic acid (EDTA), 0.5% Zwittergent 3–12 (N-dodecyl-*N*,*N*-dimethyl-3-ammonio-1-propanesulfonate) and protease inhibitor (Complete, Roche Applied Science)) for 2 h at 0 °C [41]. Lysates were centrifuged for 10 min at 2500 ×*g* and for 45 min at 31000 x g to remove nuclei and other insoluble material, respectively. Lysates were passed through a 50 μL CL-4B Sepharose column (in a standard yellow tip equipped with a filter) to pre-clear the lysate and subsequently passed through a 50 μL column containing 125 μg pan class II (Y3P) IgG coupled to protein G Sepharose [41]. The Y3P column was subsequently washed with 250 μL of lysis buffer, 250 μL of low salt buffer (20 mM Tris-Cl pH 8.0, 120 mM NaCl), 100 μL of high salt buffer (20 mM Tris-Cl pH 8.0, 1 M NaCl), and finally with 250 μL of the low salt buffer. I-Ab and peptides were eluted with 250 μL of 10% acetic acid, diluted with 1 mL of 0.1% trifluoroacetic acid (TFA) and purified by SPE (Oasis HLB, Waters) by sequential elution with 20%, 30% and 40% acetonitrile in 0.1% TFA to recover MHC peptide molecules.

2.5. Mass spectrometry

MHC peptides were analyzed by using an Easy nLC1000 (Thermo, Bremen, Germany) coupled to a Q-Exactive mass spectrometer (Thermo). The injection was done onto a homemade pre-column (100 μm × 15 mm; Reprosil-Pur C18-AQ 3 μm, Dr. Maisch, Ammerbuch, Germany) and elution *via* a homemade analytical column (15 cm × 50 μm; Reprosil-Pur C18-AQ 3 μm). The gradient was 0% to 30% solvent B (90% ACN/0.1% TFA) in 120 min. The analytical column was drawn to a tip of around 5 μm and acted as the electrospray needle of the MS source. The Q-Exactive mass spectrometer was operated in top10-mode. Parameters were as follows: full scan, 70,000 resolution, 3,000,000 AGC target, max fill time 20 ms; MS/MS, 35,000 resolution, 100,000 AGC target, 60 ms max fill time, 17,400 intensity threshold. Apex trigger was set to 1–5 s and allowed charges were 2–5. Proteome Discoverer version 2.1 was used for peptide and protein identification, using the mascot node for identification, using mascot version 2.2.04 with the UniProt/Mouse database (51,374 entries). Methionine oxidation (on methionine) and cysteinylation (on cysteine) were set as variable modification. Precursor ion mass tolerance was set to 10 ppm. MS/MS fragment tolerance was 20 mmu. ApoB100-derived peptides as proposed by the software are shown in Table S1 and were manually assessed. The identified ApoB100 peptides were screened *in silico* (www.IEDB.org) for their ability to bind to MHC-II (Table S2). The correct assignment of the candidate peptide of sequence LSQEYSGSVANEAN was confirmed by matching of the MS/MS spectrum of eluted peptide and its synthetic peptide counterpart (Fig. S1).

2.6. Liposome preparation

Liposomes were prepared by using the thin film dehydration-rehydration method, as described previously [42]. Briefly, DSPC (T_m = 54.9 °C [43]), a charged lipid (DSPG (T_m = 54.4 °C [44]), DPPS (T_m = 55 °C [45]), or DPTAP (T_m = 52.8 °C [46])) and cholesterol were dissolved in chloroform and mixed in a round-bottom flask at a molar ratio of 4:1:2 DSPC:charged lipid:cholesterol to obtain a final lipid concentration of 10 mg/mL. The chloroform was evaporated in a rotary evaporator (Rotavapor R-210, Büchi, Switzerland) for 1 h at 40 °C. The lipid film was rehydrated with 250 μg OVA323 dissolved in 1 mL Milli-Q water and homogenized by rotation at 60 °C by using glass beads. Next, the liposome dispersion was snap-frozen in liquid nitrogen, followed by freeze-drying overnight (Christ alpha 1–2 freeze-dryer, Osterode, Germany). The freeze-dried lipid cake was slowly rehydrated by using 10 mM phosphate buffer (PB), pH 7.4 at 60 °C; two volumes of 500 μL and one volume of 1000 μL PB were successively added, with intervals of 30 min between each addition. The mixture was vortexed well between each hydration step, and the resulting dispersion was kept at 60 °C for at least 1 h. The multilamellar vesicles were sized by high-pressure extrusion at 60 °C (LIPEX Extruder, Northern Lipids Inc., Canada). To obtain monodisperse liposomes, the liposome mixture was passed four times through stacked 400 nm and 200 nm pore size membranes. To separate non-encapsulated OVA323 from the liposomes, liposomes were washed by using a Vivaspin 2 centrifuge membrane concentrator (MWCO 300 kDa, Sartorius, Göttingen, Germany). DSPG-containing liposomes encapsulating the ApoB100-derived peptide p3500 were prepared in the same way as OVA323 liposomes, where the lipid film was rehydrated with 250 μg p3500 dissolved in 1 mL Milli-Q water. To prepare fluorescently labeled liposomes, 0.5 mol % of DSPC was replaced with DPPE-Rho. Liposomes were stored at 4 °C and used for further experiments within 2 weeks.

2.7. Liposome characterization

The *Z*-average diameter (Z_{ave}) and polydispersity index (PDI) of the liposomes were measured by dynamic light scattering (DLS) using a NanoZS Zetasizer (Malvern Ltd., Malvern, UK). Zeta-potential was determined by using laser Doppler electrophoresis using the same instrument. For measurements, the liposomes were diluted 100-fold in 10 mM phosphate buffer at pH 7.4 to a total volume of 1 mL. To determine the concentration of loaded OVA323, the peptide was separated from liposomes by using a modified Bligh-Dyer method, as described previously [42]. Briefly, 100 μL of aqueous liposomal dispersion or a known concentration of free peptide as control was mixed with 250 μL methanol and 125 μL chloroform and vortexed briefly. 250 μL of 0.1 M HCl and 125 chloroform was added and the mixture was vortexed again. This was then centrifuged for 5 min at 1500 rpm to separate the water-methanol phase (containing the peptide) from the chloroform phase. The upper water-methanol phase was collected and analyzed by reversed phase UPLC (Waters ACQUITY UPLC, Waters, MA, USA). For this, 5 μL of the sample was injected into a 1.7 μm BEH C18 column (2.1 × 50 mm, Waters ACQUITY UPLC, Waters, MA, USA). The column temperature and the temperature of the sample were set at 40 °C and

4 °C respectively. The mobile phases were Milli-Q water with 0.1% TFA (solvent A) and acetonitrile with 0.1% TFA (solvent B). For detection, the mobile phases were applied in a linear gradient from 5% to 95% solvent B over 5 min at a flow rate of 0.370 mL/min. Peptides were detected by absorbance at 220 nm using an ACQUITY UPLC TUV detector (Waters ACQUITY UPLC, Waters, MA, USA).

2.8. Protein corona analysis

To characterize the formation of a protein corona on liposomes, liposomes were diluted to a lipid concentration of 0.1 mg/mL and incubated for 1 h at 37 °C with FCS or 10 μg/mL C1q in PB. Liposomes were washed three times and concentrated with a Vivaspin 500 centrifuge membrane concentrator (MWCO 1000 kDa, Sartorius, Goettingen, Germany) to remove unbound proteins, leaving the 'hard' protein corona [47]. Size, PDI, and zeta-potential of liposomes were measured with a NanoZS Zetasizer (Malvern Ltd., Malvern, UK). SDS-PAGE was performed according to the manufacturer's instructions. Samples and MW standards were diluted 1:1 in reducing Laemmli buffer and 10 μL of sample was loaded per lane. Gels were stained with Coomassie Blue and analyzed by using a scanner (GS-900™, Bio-Rad, Veenendaal, the Netherlands) and Image Lab™ software (Bio-Rad, Veenendaal, the Netherlands). For WB for C1q, SDS-PAGE was first carried out as described above, and proteins were transferred by using the wet blotting method according to the manufacturer's instructions. Blots were blocked overnight at 4 °C with PBS containing 2% BSA and 0.5% polysorbate 20. Subsequently, blots were incubated for 1 h at room temperature with biotinylated anti-C1q antibody diluted 1000-fold in blocking buffer, followed by 1-h incubation at room temperature with streptavidin-HRP diluted 1000-fold in blocking buffer. An AEC staining kit was used to develop the blots, and we analyzed blots with a scanner and Image Lab™ software.

2.9. Liposome uptake by BMDCs

BMDCs were cultured as described above. After 10 days of culture, 50,000 BMDCs were plated in 96-well plates (Greiner Bio-One B.V., Alphen aan den Rijn, Netherlands) and fluorescently labeled liposomes or controls were added at a concentration of 0.1 μg/mL OVA323 in different media. To block SR-mediated uptake, 250 μg/mL poly I was added. After 4 h of incubation at 37 °C and 5% CO_2, excess liposomes were removed by washing the cells several times with IMDM. Cultures were supplemented with 20 ng/mL GM-CSF and incubated overnight. Cells were analyzed by flow cytometry (CytoFLEX S, Beckman Coulter, CA, USA). BMDCs were stained for CD11c and viability. The presence of the fluorescent label in the liposomes indicated uptake by BMDCs. Data were analyzed by using FlowJo software (Treestar, OR, USA).

2.10. In vitro Treg induction by liposome-pulsed BMDCs

Wild-type (WT) or TIM4$^{-/-}$ BMDCs were cultured as described above, and activated for 4 h with liposomes or controls in different media. Spleens were removed from OT-II mice and strained through a 70-μm cell strainer to obtain a single-cell suspension. Erythrocytes were lysed with Ammonium-Chloride-Potassium (ACK) lysis buffer (0.15 M NH_4Cl, 1 mM $KHCO_3$, 0.1 mM Na_2EDTA; pH 7.3). CD4$^+$ T cells were isolated using a CD4$^+$ T cell isolation kit (Miltenyi Biotec B.V., Leiden, Netherlands) according to the manufacturer's protocol. After incubation, BMDCs were thoroughly washed with PBS to remove any free liposomes, and 100,000 CD4$^+$ T cells were added to obtain a number ratio of 2:1 CD4$^+$ T cells:BMDCs. Co-cultures were cultured for 72 h in complete RPMI 1640 medium supplemented with 2 mM glutamine, 10% FCS, 100 U/mL penicillin/streptomycin, and 50 μM β-mercaptoethanol. Cells were stained for Thy1.2, CD4, viability, FOXP3, and Ki67, and analyzed by flow cytometry (CytoFLEX S, Beckman Coulter, CA, USA). Data were analyzed by using FlowJo software (Treestar, OR, USA).

2.11. Analysis of antigen-specific CD4$^+$ T cell responses in vivo

12-week-old male C57BL/6 mice were randomized into 5 groups. On day 0, all groups received splenocytes isolated from a female OT-II transgenic mouse equivalent to 500,000 CD45.1$^+$CD4$^+$ T cells *via* the tail vein. On day 1, mice were immunized intravenously (i.v.) with a single injection of either PBS, 1 nmol free OVA323 in PBS, or liposomes containing 1 nmol OVA323 in PBS, in a total volume of 200 μL *via* the tail vein. Seven days after immunization, a small amount of blood was collected from the mice *via* the tail. Blood samples were lysed and stained for Thy1.2, CD4, CD45.1 and viability, and samples were analyzed by flow cytometry (Cytoflex S, Beckman Coulter, Indiana, USA). On day 8, mice were sacrificed by cervical dislocation and spleens and inguinal lymph nodes (iLNs) were immediately removed. Organs were processed and stained for CD4, CD45.1, Thy1.2, viability, Ki67, CD25 and FOXP3 and measured by flow cytometry. To measure cytokine production, splenocytes were stimulated *ex vivo* with PMA (50 ng/mL) and Ionomycin (500 ng/mL). After 1-h brefeldin A (3 μg/mL) was added and cells were incubated for a further 5 h. Cells were subsequently stained for Thy1.2, CD4, CD45.1, viability, IFN-γ, IL-17, IL-4 and IL-10 and analyzed by flow cytometry.

2.12. Analysis of atherosclerosis in mice

Eight- to 14-week-old male LDLr$^{-/-}$ mice were randomized into 3 groups of 9 mice. Mice were fed a WTD for 10 weeks to induce atherosclerosis. During this time, mice were immunized at week 0, 3, 6 and 9 *via* i.p. injection with either PBS, 10 nmol of free p3500 peptide in PBS, 0.5 mg DSPG-liposomes in PBS, or 0.5 mg DSPG-liposomes containing 10 nmol of p3500 in PBS, in a total volume of 200 μL. After 10 weeks, mice were euthanized by a subcutaneous injection (120 μL) of a cocktail containing ketamine (40 mg/mL), atropine (50 μg/mL), and sedazine (6.25 mg/mL). Mice were exsanguinated and perfused with PBS. For flow cytometry, aortas were harvested and cut into small pieces. These were incubated for 30 min at 37 °C with 450 U/mL collagenase I, 250 U/mL collagenase XI, 120 U/mL DNAse, and 120 U/mL hyaluronidase, and strained through a 70-μm cell strainer to obtain a single-cell suspension. Cells were stained for Thy1.2, CD4, CD8 and viability. Hearts were harvested and fixed frozen in OCT formulation at −80 °C. Hearts were subsequently cryosectioned horizontally to the aortic axis and towards the aortic arch. Upon identification of the aortic root, defined by the trivalve leaflets, 10 μm sections were collected. Sections were stained for Oil-Red-O as previously described [48] to visualize lipid-rich plaques. Macrophages in the plaques were stained using MOMA2 staining as previously described [49]. Collagen in the plaques was stained using Sirius Red staining, as previously described [50]. All stainings were analyzed by microscopy using Leica QWin software on a Leica DM-RE microscope (Leica, Imaging Systems, UK). Briefly, the area stained positively for Oil-Red-O, expressed as μm^2, was determined for the section with the largest lesion, and the two flanking sections to estimate the average plaque size. The average percentage of macrophages in the plaque was determined by dividing the area positive for the MOMA2 staining by the total plaque area for the 3 largest subsequent sections. Sirius Red staining was visualized under polarized light [51], and the percentage of collagen was calculated by dividing the area positive for the Sirius Red staining by the total plaque area for the 3 largest subsequent sections. Blood samples were prepared for determination of serum cholesterol levels as previously described [30].

2.13. Statistical analysis

Results were analyzed using one-way or two-way ANOVA, followed by Bonferroni's multiple comparisons test and was performed using GraphPad Prism version 7.00 for Windows (GraphPad Software, CA,

Table 1
Physicochemical properties of OVA323-containing liposomes composed of 4:1:2 M ratio DSPC:charged lipid:chol.

Charged lipid	Z_{ave} (nm)[a]	PDI	Zeta-potential (mV)	% LE[b]
DSPG	167.3 ± 11.8	0.08 ± 0.04	−54.4 ± 5.5	10.6 ± 3.9
DPPS	165.4 ± 15.7	0.12 ± 0.05	−54.0 ± 6.4	14.7 ± 4.7
DPTAP	166.9 ± 14.9	0.09 ± 0.04	33.7 ± 3.7	27.6 ± 8.5

[a] *Z*-average diameter (Z_{ave}), mean ± SD, $n = 12$.
[b] %LE was calculated as the total amount of peptide before extrusion/total amount of peptide after purification * 100%.

USA).

3. Results

3.1. Preparation of liposomes

Anionic liposomes are associated with tolerance induction [36,37], although it is unclear whether this is merely due to the negative charge or the specific anionic head group.

In order to determine which anionic phospholipid would be most effective for the induction of antigen-specific Tregs, we prepared liposomes containing DSPG or DPPS, ensuring all other physicochemical characteristics like size, zeta-potential and rigidity remained similar. As a positive control for pro-inflammatory responses, we made DPTAP-containing liposomes. Liposomes were prepared with DSPC, charged lipids (DSPG, DPPS or DPTAP) and cholesterol at a molar ratio of 4:1:2 with an initial concentration of 250 μg/mL OVA323. The liposomes were around 165 nm in size and were monodisperse, with a PDI around 0.1 (Table 1). As expected, the zeta potential of the liposomes was negative for both anionic liposomal formulations and positive for the DPTAP liposomes. The loading efficiency (LE) of OVA323 was between 10 and 15% for the anionic liposomes and almost 30% for the cationic liposomes. The addition of a small amount of fluorescently labeled DPPE did not alter the liposomal properties (Table S3), and replacing OVA323 with the athero-specific ApoB100-derived peptide p3500 did not alter the properties of DSPG-liposomes (Table S4).

3.2. Liposomes induce strong antigen-specific $CD4^+$ T cell responses in mice

To determine the effect of liposomes on antigen-specific $CD4^+$ T cell expansion *in vivo*, a single immunization with OVA323-containing liposomes or free OVA323 was performed in mice, which had received an adoptive transfer of OT-II splenocytes one day prior to immunization. All liposomal formulations induced proliferation of antigen-specific $CD45.1^+CD4^+$ T cells in the blood of mice just 7 days after immunization (Fig. 1A, D, E, F, and G). In contrast, free OVA323 induced almost no antigen-specific $CD4^+$ T cell proliferation, comparable to PBS. We observed very similar results in the spleens and iLNs on day 8 (Fig. 1B and C). The antigen-specific $CD4^+$ T cell proliferation induced by cationic liposomes tended to be increased, albeit not significant compared to OVA-specific $CD4^+$ T-cell responses induced by anionic liposomes (Fig. S2).

3.3. DSPG-liposomes induce antigen-specific Tregs in vivo

To uncover the type of OVA323-specific $CD4^+$ T cells induced by the liposomes in mice, antigen-specific ($CD45.1^+CD4^+CD25^+FOXP3^+$) Tregs were measured by flow cytometry after immunization (Fig. 2A, B, and C). We found comparable percentages of non-specific Treg populations ($CD45.1^-CD4^+CD25^+FOXP3^+$) in all mice (Fig. S3). DSPG-liposomes encapsulating OVA323 induced the highest percentage of antigen-specific Tregs, which was significantly higher than the background Treg response after injection of free OVA323. Surprisingly, DPPS-liposomes were not as efficient at Treg induction as DSPG-liposomes, but they did show a non-significant increase in Tregs compared to free OVA323. DPTAP-liposomes did not alter Treg responses as compared to the background. We also measured antigen-specific intracellular cytokine responses by flow cytometry after restimulation with PMA and ionomycin (Fig. 2D, E, F, and G). DPTAP-liposomes greatly increased pro-inflammatory cytokine production (interferon (IFN)-γ and IL-17) of the antigen-specific $CD4^+$ T cells, while both anionic liposomes induced almost no production of these cytokines. There were no differences in IL-4 or IL-10 production in any of the groups.

3.4. Anionic liposomes attract C1q from serum and are taken up by SRs

While both anionic liposomal formulations had similar physicochemical properties and could induce Tregs, DSPG-containing liposomes were clearly more potent. The cationic DPTAP liposomes induced no Tregs. We hypothesized that a protein corona around the liposomes could be responsible for the differences in *in vivo* immunological responses. To assess the formation of a protein corona, we incubated the anionic liposomes in FCS for 1 h at 37 °C and washed them to remove any unbound proteins, leaving the 'hard' protein corona. SDS-PAGE analysis showed that the liposomes attract proteins from FCS (Fig. S4A). Several serum proteins can bind to nanoparticles, including complement proteins [52]. Of these complement proteins, C1q is especially interesting since it can bind to various receptors [53]. Notably, binding of C1q to PS on apoptotic cells leads to recognition and clearance by phagocytic cells *via* SRs [54–56]. To test whether the protein corona or C1q is important for uptake of liposomes by BMDCs and Treg induction, we measured uptake of fluorescently labeled liposomes by BMDCs in the absence of serum, or in medium containing either 8% FCS or C1q. We also assessed OT-II $FOXP3^+Ki67^+CD4^+$ T cell induction by these BMDCs. Both DSPG- and DPPS-liposomes showed an uptake of < 10% in the absence of FCS or C1q, however, the uptake of DPPS-liposomes was around 10-fold lower in this condition (Fig. 3A). Addition of C1q or FCS significantly increased uptake of both liposomes, with DSPG-liposomes showing significantly higher uptake than DPPS-liposomes in normal serum conditions at the concentration of lipids we examined (Fig. 3A). Moreover, for DSPG-liposomes, depletion of C1q from serum significantly reduced uptake, which was remedied by reconstituting C1q (Fig. S5). Liposomes in the presence of serum significantly increased Treg induction compared to serum-free conditions (Fig. 3B). The *in vitro* data supports the *in vivo* findings, *i.e.*, in the presence of serum, both liposomes enhanced Treg induction compared to free OVA323, and DSPG liposomes were more potent. It should be noted that, although DCs can produce C1q [57], the short incubation time of 4 h should not allow for a significant production of C1q. We also assessed whether TIM4, a known receptor for apoptotic cells that plays an important role in atherosclerosis [58], plays a role in mediating the uptake of our liposomes and induction of Tregs. However, $TIM4^{-/-}$ BMDCs showed no differences in liposome uptake and Treg induction compared to WT BMDC (Fig. S6).

Importantly, C1q is present in FCS and in the protein corona of both DSPG- and DPPS-liposomes, as measured by SDS and WB (Fig. 4A, Fig. S4B). To test the effect of FCS and C1q binding to the liposomes on their physicochemical properties, we incubated liposomes either with FCS in PB or with C1q in PB, washed them, and analyzed them using DLS. Either condition significantly increased the size of both DSPG- and DPPS-liposomes as compared to a protein-free medium. However, there were no signs of severe aggregation of liposomes, as the size remained below 200 nm for all groups (Fig. 4B, E, and F). For both liposomal formulations, C1q binding moderately but significantly increased PDI and reduced the negative zeta-potential of the liposomes. FCS binding enhanced this effect even further (Fig. 4C and D).

As C1q has been reported to mediate SR-mediated uptake, we evaluated the role of SR-mediated uptake of liposomes by BMDCs by measuring uptake of fluorescently labeled liposomes in the presence of

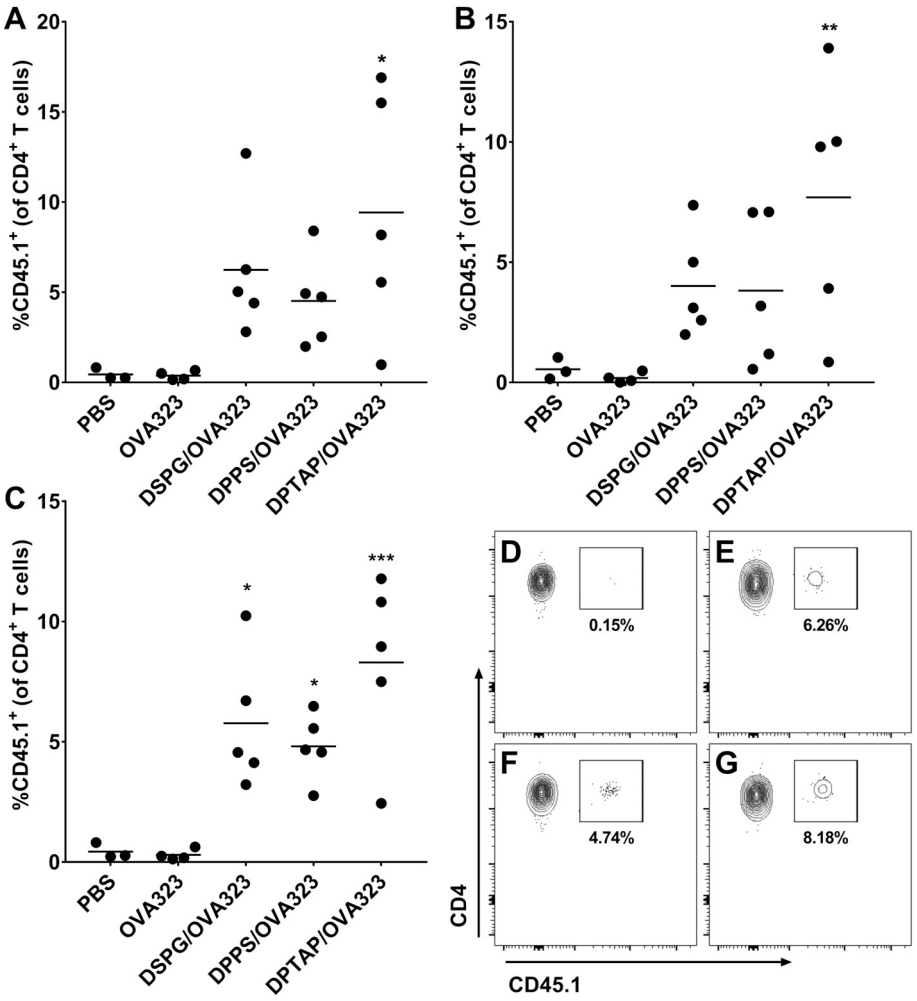

Fig. 1. Expansion of OVA323-specific $CD4^+$ T cells in blood, spleens, and iLNs of mice after i.v. injection of OVA323-containing liposomes. (A) $CD45.1^+$ $CD4^+$ T cells in blood (day 7), (B) inguinal LNs (day 8) and (C) spleen (day 8) of mice after immunization with DSPG-, DPPS-, or DPTAP-liposomes containing the OVA323 peptide, or PBS or free OVA323 peptide. Representative flow cytometry plots of pre-gated $CD4^+$ T-cells in the blood mice 7 days after immunization with (D) free OVA323, (E) DSPG/OVA323-, (F) DPPS/OVA323-, and (G) DPTAP/OVA323-liposomes. $*p < .05$, $**p < .01$, compared to free OVA323 determined by one-way ANOVA and Bonferroni's multiple comparisons test. No significant differences were found between the different liposomal formulations. Representative example of 2 independent experiments.

poly I, a non-selective SR antagonist [59], in both medium containing 8% FCS or serum-free medium Blocking of SR-mediated uptake in the presence of serum reduced uptake of both DSPG- and DPPS-liposomes to the levels of "- serum", indicating that SRs are responsible for the uptake of most of the liposomes by BMDCs under normal serum conditions (Fig. 5). The addition of poly I did not alter the uptake of liposomes in serum-free conditions, suggesting that bare liposomes did not interact with SRs (Fig. 5).

3.5. DSPG-liposomes encapsulating an atherosclerosis-specific peptide significantly reduce plaque formation and increase plaque stability in atherosclerotic mice

Tolerance induction against atherosclerosis using peptides targeted against the main antigen in atherosclerosis, LDL, has yielded some success [23–28]. We hypothesized that encapsulation of an atherosclerosis-specific peptide in DSPG-liposomes would reduce atherosclerosis progression more efficiently than the free peptide, *via* induction of antigen-specific Tregs. The protein surrounding LDL, ApoB100, is a large protein (515 kDa in humans, 509 kDa in mice) containing several potential $CD4^+$ T cell epitopes. To identify a relevant ApoB100 peptide for immunization, we eluted MHC-II restricted peptides from BMDCs exposed to hypercholesterolemic serum. We identified several ApoB100-derived peptides using our peptidomics strategy (Table S1). Based on the predicted MHC-II binding (Table S2) we selected the peptide $ApoB100_{3500–3514}$ (p3500) and successfully loaded it into DSPG-liposomes (Table S4). $LDLr^{-/-}$ mice on a WTD were selected as a model for diet-induced atherosclerosis [12]. The mice were fed a WTD for 10 weeks, during which they were injected i.p. four times with PBS, 10 nmol of free p3500 or 10 nmol of p3500 encapsulated in DSPG-liposomes (DSPG/p3500-liposomes). Neutral lipid staining (Oil-Red-O) of the aortic valve area of the heart, which is used to quantify the lipid-rich atherosclerotic lesion, showed that treatment with p3500-loaded DSPG-liposomes significantly reduced the lesion area by 50% (Fig. 6A and B). As expected, all mice gained weight due to the WTD, but there were no differences between the groups (Fig. 6C). Similarly, serum cholesterol levels were elevated in all groups because of the WTD. Interestingly, only the group of mice that received the DSPG/p3500 treatment had significantly lower levels of serum cholesterol compared to the PBS control group (Fig. 6D). The aortic sections were further stained for macrophage content, which is an indicator of immune activation [60]. Differences in macrophage content between the groups were not significant, although there was a trend towards lower macrophage content in the mice immunized with liposomes (Fig. 6B and E), which could be (partially) responsible for the reduction in plaque size. Furthermore, there were significantly fewer $CD8^+$ T cells present in the aorta of mice injected with liposomes (Fig. S7B). Levels of the inflammatory $CCR2^+Ly\text{-}6C^{hi}$ monocytes were unchanged in the blood of mice in all groups (Fig. S8A), further indicating that there was no increased inflammation. Finally, the collagen content in the lesions was assessed, as an indication of lesion stability [51]. Only the mice receiving DSPG/p3500 presented with a higher collagen content in their lesions (Fig. 6B and F), suggesting a more stable plaque. Total Treg levels were the same in all groups (Fig. S8B).

Previous work suggests injection of PS-containing liposomes can affect atherosclerosis development [38]. Therefore we investigated

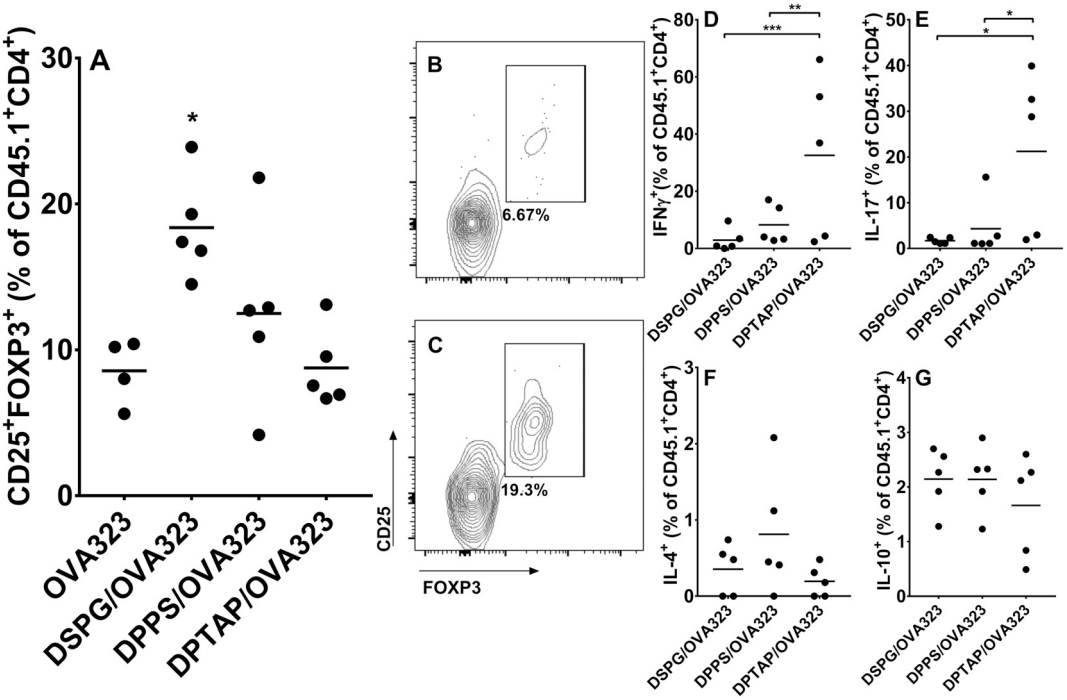

Fig. 2. Induction of OVA323-specific immune responses in iLNs and spleens of mice 8 days after i.v. injection of OVA323-containing liposomes. (A) $CD25^+FOXP3^+CD4^+$ T cells from adoptive transfer of $CD4^+$ T cells from an OT-II mouse were detected in iLNs of WT mice after immunization with free OVA323, or DSPG-, DPPS- or DPTAP-liposomes containing OVA323 peptide. Representative flow cytometry plots of pre-gated $CD45.1^+CD4^+$ T-cells in the iLNs of a mouse 8 days after immunization with (B) DPTAP, or (C) DSPG liposomes. Splenocytes were incubated for 6 h with PMA + ionomycin and brefeldin A, and subsequently, (D) IFNγ, (E) IL-17, (F) IL-4 and (G) IL-10 production by antigen-specific $CD45.1^+CD4^+$ T cells was analyzed by flow cytometry. Graphs show mean, *p < .05, **p < .01 determined by one-way ANOVA and Bonferroni's multiple comparisons tests. Representative of 2 independent experiments.

whether empty DSPG-liposomes may have mediated the decrease serum cholesterol levels and inhibition of atherosclerosis. However, we found no differences in serum cholesterol, plaque size, or immune activation upon immunization with DSPG liposomes compared to PBS (Fig. S9). Thus, the results suggest that DSPG/p3500-liposomes are able to reduce the growth of atherosclerotic lesions, lower serum cholesterol levels, and stabilize atherosclerotic plaques.

4. Discussion & conclusion

Atherosclerosis is the main underlying pathology for cardiovascular disease and is one of the leading causes of death worldwide [1]. While vaccination against atherosclerosis has been successful in murine models [23–28], a major challenge is the induction of antigen-specific Tregs in a safe and effective way. Here we introduce DSPG-liposomes as a peptide antigen carrier to induce regulatory T-cells and as a potential vaccine against atherosclerosis. Whereas DPTAP-liposomes can induce strong pro-inflammatory responses, we hypothesized that DSPG- and DPPS-liposomes lead to immune suppression because of their similarity to apoptotic cells. OVA323-containing liposomes were prepared with high-T_m lipids, since rigid liposomes have been shown to enhance APC uptake [61] and activation [62], and would, therefore, be more potent at inducing T cell responses compared to fluid-state liposomes. We show that all liposomes induced expansion of OVA323-specific T cells *in*

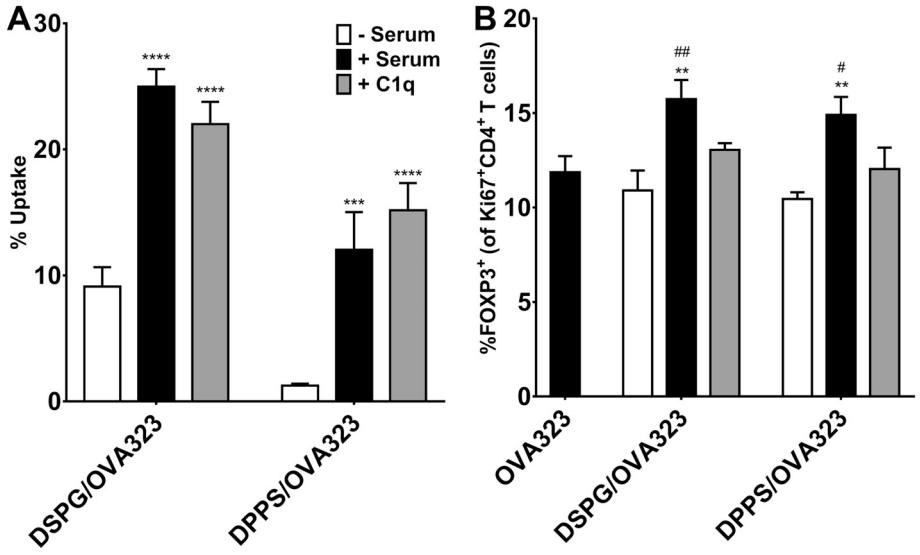

Fig. 3. Effect of C1q and FCS on *in vitro* uptake by BMDCs and subsequent antigen-specific Treg induction. (A) Percentage of DCs which have taken up fluorescently labeled OVA323-loaded DSPG- or DPPS-containing liposomes after 4 h incubation, as measured by flow cytometry. Cells were incubated with liposomes either in serum-free IMDM (white bars), in IMDM supplemented with FCS (black bars) or in IMDM supplemented with 10 μg/mL C1q (gray bars). (B) OT-II $FOXP3^+Ki67^+CD4^+$ T cells induced after 3 days co-culture with BMDCs exposed to conditions shown in (A). Graph shows mean ± SD (n = 3), * shows comparison to "- serum" condition within liposome group, # compares to free OVA323 + serum. ** p < .01, *** p < .001, **** p < .0001, # p < .05, ## p < .01 determined by one-way ANOVA and Bonferroni's multiple comparisons test.

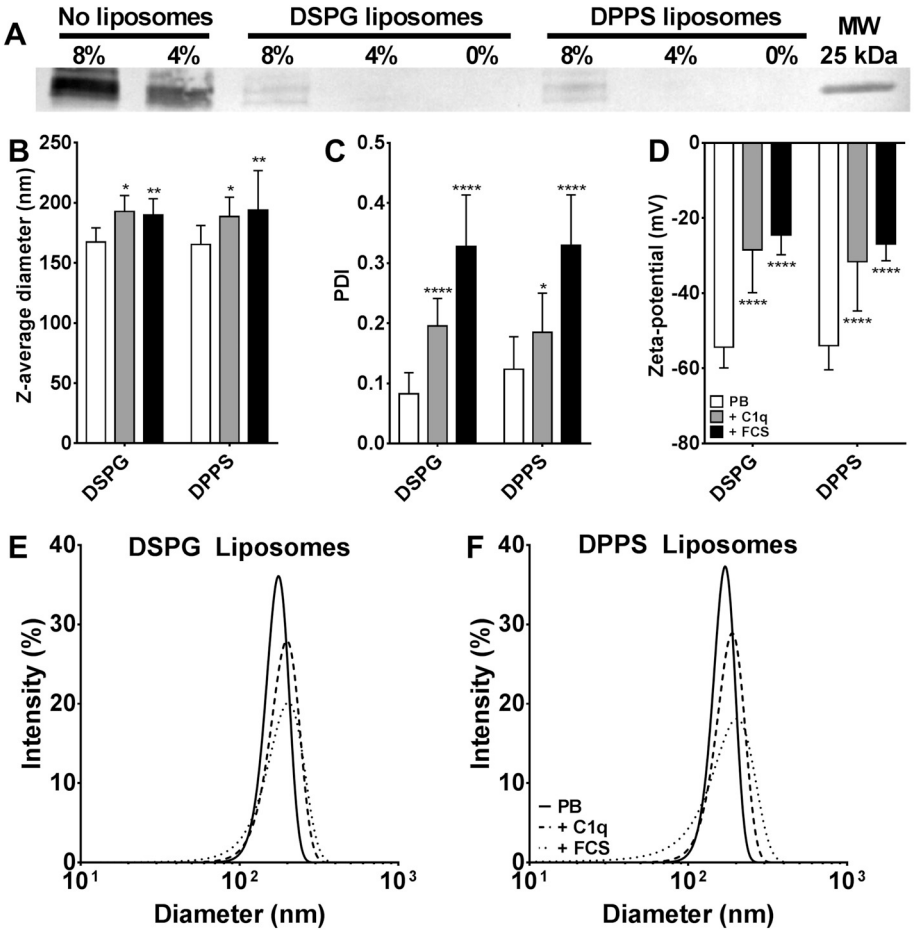

Fig. 4. Binding of C1q and FCS components to DSPG- and DPPS-liposomes Liposomes were incubated with 8% or 4% FCS for 1 h at 37 °C and subsequently washed thoroughly to remove all unbound proteins, leaving only the protein corona. (A) WB of C1q after SDS-PAGE under reducing conditions. Percentages indicate the concentration (*v*/v) of FCS in PB. FCS in PB (no liposomes) was included as a control. Complete blot is shown in Fig. S3. (B) Z-average diameter, (C) PDI, and (D) zeta-potential of samples in PB (white bars), with bound C1q (gray bars), or with bound FCS (black bars). (E and F) Representative Gaussian-smoothed intensity-weighted size distribution of DSPG- and DPPS-liposomes in PB (solid lines), with bound C1q (dashed lines) or with bound FCS (dotted lines). (F) Bar graphs show mean ± SD (n = 3) *p < .05, **p < .01, ****p < .0001, compared to PB, determined by two-way ANOVA and Bonferroni's multiple comparisons tests.

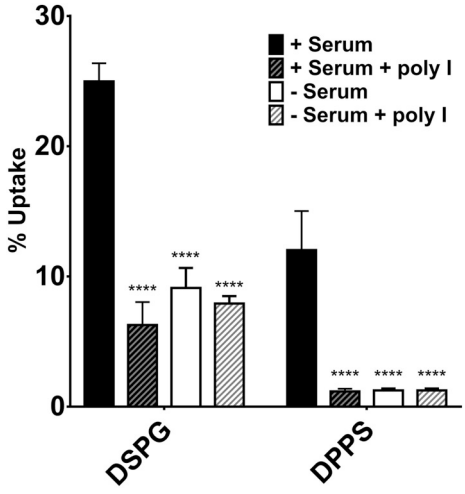

Fig. 5. Effect of SR blocking on *in vitro* uptake of fluorescently labeled anionic liposomes encapsulating OVA323 by BMDCs. Percentage of DCs which have taken up fluorescently labeled OVA323-loaded DSPG- or DPPS-containing liposomes after 4 h incubation, as measured by flow cytometry. Cells were incubated with liposomes in IMDM supplemented with FCS without SR blocking (black bars) or with SR blocking using 250 μg/mL poly I (black/Gy bars), or in serum-free IMDM without poly I (white bars) or with poly I (white/Gy bars). Graph shows mean ± SD (n = 3), ****p < .0001, compared to + serum within liposome group, determined by two-way ANOVA and Bonferroni's multiple comparisons tests.

vivo. The cationic liposomes induced pro-inflammatory cytokines, which we have also previously observed [42]. Only DSPG-containing liposomes induced significantly higher numbers of $CD25^+FOXP3^+CD4^+$ Tregs compared to free OVA323 in mice. This was surprising since PS-containing liposomes have been reported to induce antigen-specific Tregs in a type I diabetes model [36]. In accordance with our study, however, IL-10 and IL-4 responses were also unchanged in the diabetes model [36]. A head-to-head comparison of the effect of PS or PG liposomes complexed with Factor VIII (FVIII) *in vitro* showed that PS liposomes significantly reduced CD86 and CD40 expression, important co-activating molecules, in DCs as compared to free FVIII, while PG liposomes did not [63]. This supports our finding that DSPG liposomes have a higher potency to expand T cells. Unfortunately, T cell proliferation was only measured for PS liposomes, and Treg levels were not measured in the aforementioned study [63]. We show that DSPG-liposomes are more effectively taken up by BMDCs *in vitro* than DPPS-liposomes, which could explain their higher potency to induce Treg. Regardless, uptake of both liposomes was low (< 30%), which has been observed previously, most likely due to unfavorable electrostatic interactions with the negatively charged cell surface [64]. The mechanism of uptake could also be responsible for the potency of the DSPG-liposomes. *In vitro* and *in vivo*, liposomes interact with proteins in the physiological medium, resulting in the formation of a protein corona around the liposomes. Accordingly, we observed that proteins from serum attached to the liposomes and that the presence of serum was required for efficient uptake by BMDCs and subsequent Treg induction. This is in line with other studies that have shown the protein corona to be essential for the biological function of particles [65]. As mentioned above, several SRs could be responsible for anionic liposome uptake, and SR-mediated uptake may lead to immune suppression [66]. We found a significant reduction of uptake for both PG- and PS-

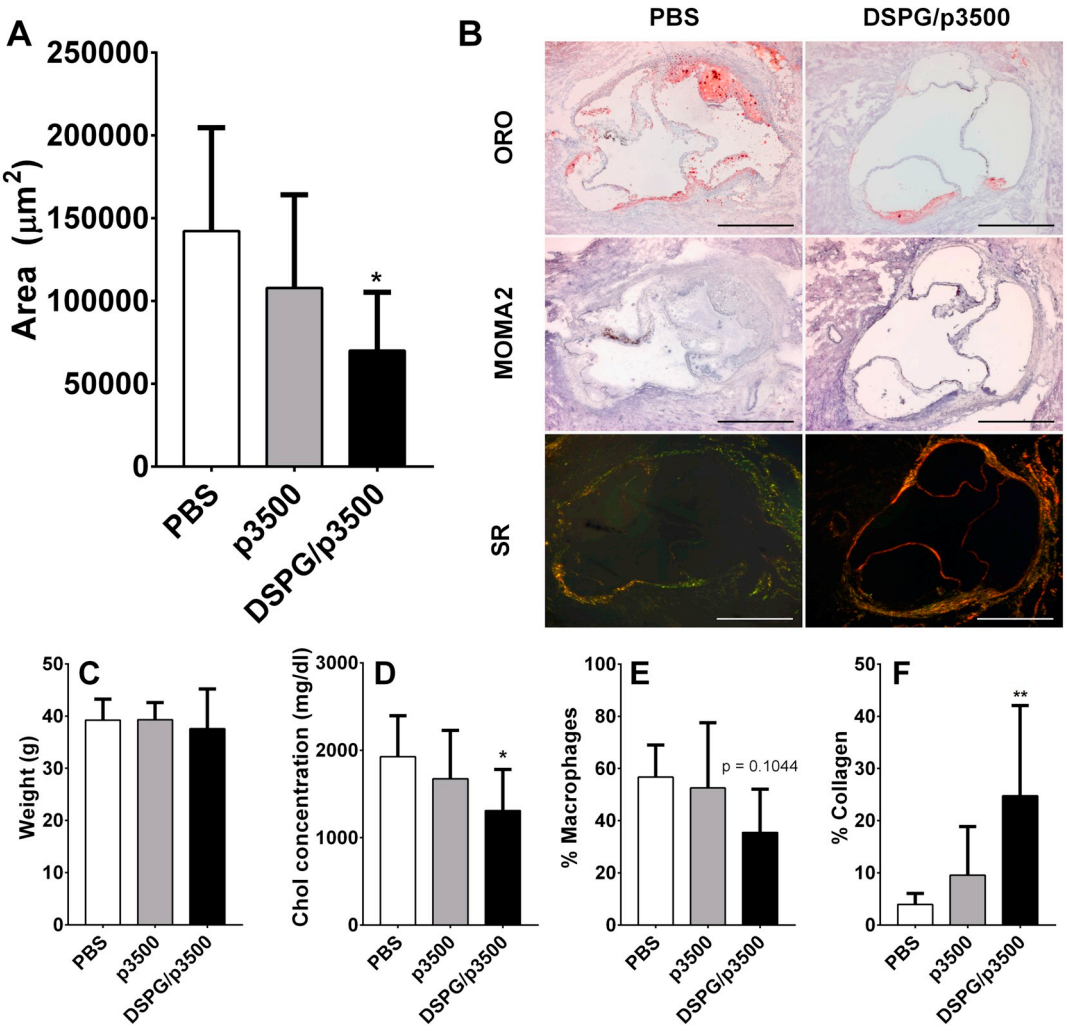

Fig. 6. Histological analysis of lesion formation in the aortic valve area of LDLr$^{-/-}$ mice. LDLr$^{-/-}$ mice on a WTD were administered either with PBS, 10 nmol free p3500 or 10 nmol p3500 encapsulated in DSPG-liposomes *via* i.p. injection every 3 weeks for 10 weeks on a WTD. (A) Lesion area as determined by Oil-Red-O staining. (B) Representative images of sections of the aortic valve area in a mouse receiving PBS or DSPG/p3500-liposomes. Stainings shown are Oil-Red-O (ORO) and hematoxylin, monocyte/macrophage marker (MOMA2), and Sirius Red. In the Sirius Red staining, Type I collagen fibers are stained red, while Type III collagen fibers appear green. (C) The weight of mice at sacrifice. (D) Serum cholesterol levels of mice at sacrifice. (E) Percentage of macrophage area relative to total lesion area as determined by MOMA2 staining. (F) Percentage of collagen area relative to total lesion area as determined by Sirius Red staining. Graphs show mean ± SD (n = 9), *p < .05, **p < .01 determined by one-way ANOVA and Bonferroni's multiple comparisons tests. (For interpretation of the references to colour in this figure legend, the reader is referred to the web version of this article.)

liposomes in the presence of serum when SR-mediated uptake was blocked, which was not observed in serum-free conditions, suggesting that formation of a protein corona is required for SR interactions. PS-liposomes were entirely dependent on SR function for uptake, whereas PG-liposomes appear to have at least one additional mechanism of uptake, and could even interact directly with cells, as there was still uptake in serum-free conditions. There is evidence of binding of anionic lipids to apoptotic receptors [37,67–71]. We have so far excluded TIM4 as a receptor for PG- or PS-liposome uptake and Treg induction.

Since the serum protein C1q can bind to PS on apoptotic cells and lead to clearance *via* SRs [54–56,72], we tested whether C1q present in the protein corona of the liposomes was responsible for SR-mediated uptake and Treg induction. C1q forms part of the C1 complex that is required for triggering of the classical complement pathway but can also regulate immunity [53,73]. Complement activation seems to be dependent on the structure of C1q; when it binds to IgG1, C1q has a different conformation than when it binds directly to PS exposed on the cell surface or liposomes [74]. Moreover, there is evidence of viruses binding C1q as a bridging molecule to evade the immune system and enhance infection [75–77]. C1q deficiency, either genetic [78] or *via* anti-C1q autoantibodies [72], can lead to symptoms almost identical to systemic lupus erythematosus (SLE). Several other autoimmune disorders have been associated with a dysregulation of the complement system and specifically C1q deficiencies, including atherosclerosis [79]. We show that C1q is present in the protein corona and binds to anionic liposomes. This is in accordance with other reports of C1q binding to PS- [70] and PG-containing liposomes [80]. The addition of C1q in serum-free conditions completely restored the uptake of both PG- and PS-liposomes. Furthermore, depletion of C1q significantly reduced uptake of PG-liposomes. Therefore, another explanation for the higher potency of DSPG-liposomes could be that they attract C1q from the circulation more efficiently than DPPS-liposomes. Since C1q cannot bind to free PS or PG [70], the density and repetitiveness of anionic head groups on liposomes may be an important parameter that affects C1q binding [81]. The molar ratios of the lipids used in this study were identical, so this would not affect binding of C1q. It has also been suggested that the electrostatic charge of the liposomes is an important parameter for binding [80,82], or that the chemical structure of the lipids is crucial [83]. In this work, the zeta-potential was the same for both liposomal formulations, leaving the structure of the phospholipid

headgroup as the only differing factor.

Since there was a clear role for C1q in the uptake of the liposomes, we hypothesized that this may also influence Treg skewing. While we did observe that the addition of C1q increases Treg responses compared to serum-free conditions, this was not significant. Similarly, Clarke et al. showed that, while C1q tolerizes macrophages (increased PD-L1 and PD-L2, decreased CD40) and DCs (increased PD-L2 and decreased CD86), there was only a trend towards higher Treg responses [84]. This suggests that C1q is partially responsible for the Treg induction of both DSPG- and DPPS-liposomes, but the protein corona likely contains more components that help to induce Tregs.

Finally, we tested whether our most tolerogenic formulation was able to prevent disease progression in atherosclerosis. We immunized atherosclerotic mice with 10 nmol of our newly identified ApoB100-derived peptide (p3500), either free or encapsulated inside DSPG-liposomes. We observed a highly significant decrease in atherosclerotic lesion size of 50% only in the group that was immunized with the p3500 liposomes. Interestingly a previous study where ApoE$^{-/-}$ mice received a similar MHC-II restricted ApoB100-derived peptide ($ApoB100_{3501–3516}$) in complete Freund's adjuvant (CFA), and four booster injections in incomplete Freund's adjuvant (IFA) showed a comparable reduction in aortic plaque formation of 60% [23]. In addition, there were no changes in Treg populations upon this treatment [23], which is similar to our findings. In a more recent paper by the same group using a novel ApoB100-derived peptide and custom tetramers, antigen-specific Tregs were found [28]. This is in spite of that fact that CFA and IFA are not designed for tolerogenic responses; in fact, they generally elicit strong Th1 and Th2 responses [85]. This may explain why this previous study required a 3-fold higher peptide dose to induce the same atheroprotective effect we report. Moreover, because of their high toxicity, use of CFA or IFA in humans is strongly discouraged [85]. Unfortunately, we were unable to measure p3500-specific Tregs in this atherosclerosis study, due to lack of specific tetramers, however we did exclude the possibility that that protective effect was mediated by empty DSPG liposomes.

We further observed a significant decrease in serum cholesterol levels in mice receiving DSPG/p3500 treatment. It has been shown that depletion of Tregs increased cholesterol levels in LDLr$^{-/-}$ mice [86], while *in vivo* Treg expansion in LDLr$^{-/-}$ mice reduced cholesterol levels [87], so this decrease in cholesterol levels could be caused by an increase in the number of antigen-specific Tregs. Finally, an increase in collagen content in the lesions of mice that received liposomes indicated more stable lesions. In accordance with this, treatment of ApoE$^{-/-}$ mice with Tregs decreased lesion size and lesion macrophage content while increasing lesion collagen content [88].

Collectively, these data show that we were able to induce high numbers of antigen-specific CD25^{+}FOXP3^{+}CD4^{+} Tregs in mice after a single injection of DSPG-containing liposomes. Furthermore, our peptidomics strategy was able to identify a novel ApoB100-derived peptide to be used for vaccination against atherosclerosis. We show that DSPG-liposomes, only when loaded with the ApoB100-derived peptide, significantly reduced lesion size, lowered serum cholesterol levels, and stabilized lesions in a murine model of atherosclerosis. Therefore, DSPG-liposomes can be a useful delivery vehicle for the induction of antigen-specific Tregs for the treatment of atherosclerosis and other autoimmune diseases.

Funding

This work was supported by the Netherlands CardioVascular Research Initiative: the Dutch Heart Foundation, Dutch Federation of University Medical Centers, the Netherlands Organization for Health Research and Development, and the Royal Netherlands Academy of Sciences for the GENIUS project “Generating the best evidence-based pharmaceutical targets for atherosclerosis” (CVON2011-19).

Declaration of interest

None.

Acknowledgments

We thank A. C. Foks, I. Bot, and R. Martins Cardoso for technical assistance during animal studies. We thank S. G. Romeijn and G. M. C. Janssen for assistance with analytical measurements.

Appendix A. Supplementary data

Supplementary data to this article can be found online at https://doi.org/10.1016/j.jconrel.2018.10.028.

References

[1] H. Wang, M. Naghavi, C. Allen, R.M. Barber, Z.A. Bhutta, A. Carter, ... C.J.L. Murray, Global, regional, and national life expectancy, all-cause mortality, and cause-specific mortality for 249 causes of death, 1980–2015: a systematic analysis for the global burden of disease study 2015, Lancet 388 (2016) 1459–1544.
[2] A. Pirillo, G.D. Norata, A.L. Catapano, Lox-1, Oxldl, and atherosclerosis, Mediat. Inflamm. 2013 (2013) 152786.
[3] P. Libby, Inflammation in atherosclerosis, Arterioscler. Thromb. Vasc. Biol. 32 (2012) 2045–2051.
[4] I. Tabas, A.H. Lichtman, Monocyte-macrophages and T cells in atherosclerosis, Immunity 47 (2017) 621–634.
[5] A.C. Foks, A.H. Lichtman, J. Kuiper, Treating atherosclerosis with regulatory T cells, Arterioscler. Thromb. Vasc. Biol. 35 (2015) 280–287.
[6] H. Douna, J. Kuiper, Novel B-cell subsets in atherosclerosis, Curr. Opin. Lipidol. 27 (2016) 493–498.
[7] S. Sakaguchi, T. Yamaguchi, T. Nomura, M. Ono, Regulatory T cells and immune tolerance, Cell 133 (2008) 775–787.
[8] Z. Mallat, H. Ait-Oufella, A. Tedgui, Regulatory T-cell immunity in atherosclerosis, Trends Cardiovasc. Med. 17 (2007) 113–118.
[9] C. Keijzer, R. van der Zee, W. van Eden, F. Broere, Treg inducing adjuvants for therapeutic vaccination against chronic inflammatory diseases, Front. Immunol. 4 (2013) 245.
[10] M.A. Atkinson, G.S. Eisenbarth, A.W. Michels, Type 1 Diabetes, Lancet 383 (2014) 69–82.
[11] H.F. McFarland, R. Martin, Multiple sclerosis: a complicated picture of autoimmunity, Nat. Immunol. 8 (2007) 913–919.
[12] G.K. Hansson, A. Hermansson, The immune system in atherosclerosis, Nat. Immunol. 12 (2011) 204–212.
[13] A.E. Coutinho, K.E. Chapman, The anti-inflammatory and immunosuppressive effects of glucocorticoids, recent developments and mechanistic insights, Mol. Cell. Endocrinol. 335 (2011) 2–13.
[14] T.A. Barr, P. Shen, S. Brown, V. Lampropoulou, T. Roch, S. Lawrie, ... D. Gray, B. Cell Depletion, Therapy ameliorates autoimmune disease through ablation of Il-6-producing B cells, J. Exp. Med. 209 (2012) 1001–1010.
[15] L. Chatenoud, J.A. Bluestone, Cd3-specific antibodies: a portal to the treatment of autoimmunity, Nat. Rev. Immunol. 7 (2007) 622–632.
[16] T. Shoji, Y. Nishizawa, M. Fukumoto, K. Shimamura, J. Kimura, H. Kanda, ... H. Morii, Inverse relationship between circulating oxidized low density lipoprotein (Oxldl) and anti-Oxldl antibody levels in healthy subjects, Atherosclerosis 148 (2000) 171–177.
[17] S. Stemme, B. Faber, J. Holm, O. Wiklund, J.L. Witztum, G.K. Hansson, T lymphocytes from human atherosclerotic plaques recognize oxidized low density lipoprotein, Proc. Natl. Acad. Sci. U. S. A. 92 (1995) 3893–3897.
[18] G.N. Fredrikson, B. Hedblad, G. Berglund, R. Alm, M. Ares, B. Cercek, ... J. Nilsson, Identification of immune responses against aldehyde-modified peptide sequences in Apob associated with cardiovascular disease, Arterioscler. Thromb. Vasc. Biol. 23 (2003) 872–878.
[19] P. Sjogren, G.N. Fredrikson, A. Samnegard, C.G. Ericsson, J. Ohrvik, R.M. Fisher, ... A. Hamsten, High plasma concentrations of autoantibodies against native peptide 210 of Apob-100 are related to less coronary atherosclerosis and lower risk of myocardial infarction, Eur. Heart J. 29 (2008) 2218–2226.
[20] B. Fagerberg, U. Prahl Gullberg, R. Alm, J. Nilsson, G.N. Fredrikson, Circulating autoantibodies against the apolipoprotein B-100 peptides P45 and P210 in relation to the occurrence of carotid plaques in 64-year-old women, PLoS One 10 (2015) e0120744.
[21] X. Zhou, G. Caligiuri, A. Hamsten, A.K. Lefvert, G.K. Hansson, Ldl immunization induces T-cell–dependent antibody formation and protection against atherosclerosis, Arterioscler. Thromb. Vasc. Biol. 21 (2001) 108.
[22] A. Schiopu, J. Bengtsson, I. Soderberg, S. Janciauskiene, S. Lindgren, M.P. Ares, ... G.N. Fredrikson, Recombinant human antibodies against aldehyde-modified apolipoprotein B-100 peptide sequences inhibit atherosclerosis, Circulation 110 (2004) 2047–2052.
[23] K. Tse, A. Gonen, J. Sidney, H. Ouyang, J.L. Witztum, A. Sette, ... K. Ley, Atheroprotective vaccination with Mhc-Ii restricted peptides from Apob-100, Front.

Immunol. 4 (2013) 493.
[24] R. Klingenberg, M. Lebens, A. Hermansson, G.N. Fredrikson, D. Strodthoff, M. Rudling, ... G.K. Hansson, Intranasal immunization with an apolipoprotein B-100 fusion protein induces antigen-specific regulatory T cells and reduces atherosclerosis, Arterioscler. Thromb. Vasc. Biol. 30 (2010) 946–952.
[25] O. Herbin, H. Ait-Oufella, W. Yu, G.N. Fredrikson, B. Aubier, N. Perez, ... Z. Mallat, Regulatory T-cell response to apolipoprotein B100-derived peptides reduces the development and progression of atherosclerosis in mice, Arterioscler. Thromb. Vasc. Biol. 32 (2012) 605–612.
[26] G.N. Fredrikson, I. Soderberg, M. Lindholm, P. Dimayuga, K.Y. Chyu, P.K. Shah, J. Nilsson, Inhibition of atherosclerosis in Apoe-null mice by immunization with Apob-100 peptide sequences, Arterioscler. Thromb. Vasc. Biol. 23 (2003) 879–884.
[27] G.N. Fredrikson, H. Bjorkbacka, I. Soderberg, I. Ljungcrantz, J. Nilsson, Treatment with Apo B peptide vaccines inhibits atherosclerosis in human Apo B-100 Transgenic mice without inducing an increase in peptide-specific antibodies, J. Intern. Med. 264 (2008) 563–570.
[28] T. Kimura, K. Kobiyama, H. Winkels, K. Tse, J. Miller, M. Vassallo, ... K. Ley, Regulatory Cd4+ T cells recognize Mhc-Ii-restricted peptide epitopes of apolipoprotein B, Circulation 138 (11) (2018) 1130–1143 .
[29] G.H. van Puijvelde, A.D. Hauer, P. de Vos, R. van den Heuvel, M.J. van Herwijnen, R. van der Zee, ... J. Kuiper, Induction of oral tolerance to oxidized low-density lipoprotein ameliorates atherosclerosis, Circulation 114 (2006) 1968–1976.
[30] V. Frodermann, G.H. van Puijvelde, L. Wierts, H.M. Lagraauw, A.C. Foks, P.J. van Santbrink, ... S.C. de Jager, Oxidized low-density lipoprotein-induced apoptotic dendritic cells as a novel therapy for atherosclerosis, J. Immunol. 194 (2015) 2208–2218.
[31] A. Hermansson, D.K. Johansson, D.F.J. Ketelhuth, J. Andersson, X. Zhou, G.K. Hansson, Immunotherapy with tolerogenic apolipoprotein B-100-loaded dendritic cells attenuates atherosclerosis in hypercholesterolemic mice, Circulation 123 (2011) 1083–1091.
[32] K.L. Habets, G.H. van Puijvelde, L.M. van Duivenvoorde, E.J. van Wanrooij, P. de Vos, J.W. Tervaert, ... J. Kuiper, Vaccination using oxidized low-density lipoprotein-pulsed dendritic cells reduces atherosclerosis in Ldl receptor-deficient mice, Cardiovasc. Res. 85 (2010) 622–630.
[33] V.K. Raker, M.P. Domogalla, K. Steinbrink, Tolerogenic dendritic cells for regulatory T cell induction in man, Front. Immunol. 6 (2015) 569.
[34] B.S. Pattni, V.V. Chupin, V.P. Torchilin, New developments in liposomal drug delivery, Chem. Rev. 115 (2015) 10938–10966.
[35] S. Nagata, R. Hanayama, K. Kawane, Autoimmunity and the clearance of dead cells, Cell 140 (2010) 619–630.
[36] I. Pujol-Autonell, A. Serracant-Prat, M. Cano-Sarabia, R.M. Ampudia, S. Rodriguez-Fernandez, A. Sanchez, ... M. Vives-Pi, Use of autoantigen-loaded phosphatidylserine-liposomes to arrest autoimmunity in type 1 diabetes, PLoS One 10 (2015) e0127057.
[37] G.C. Ramos, D. Fernandes, C.T. Charão, D.G. Souza, M.M. Teixeira, J. Assreuy, Apoptotic mimicry: phosphatidylserine liposomes reduce inflammation through activation of peroxisome proliferator-activated receptors (Ppars) in vivo, Br. J. Pharmacol. 151 (2007) 844–850.
[38] H. Hosseini, Y. Li, P. Kanellakis, C. Tay, A. Cao, P. Tipping, ... T. Kyaw, Phosphatidylserine liposomes mimic apoptotic cells to attenuate atherosclerosis by expanding polyreactive Igm Producing B1a lymphocytes, Cardiovasc. Res. 106 (2015) 443–452.
[39] E.M. Varypataki, N. Benne, J. Bouwstra, W. Jiskoot, F. Ossendorp, Efficient eradication of established tumors in mice with cationic liposome-based synthetic long-peptide vaccines, Cancer Immunol. Res. 5 (2017) 222–233.
[40] C. Barnier Quer, A. Elsharkawy, S. Romeijn, A. Kros, W. Jiskoot, Cationic liposomes as adjuvants for influenza hemagglutinin: more than charge alone, Eur. J. Pharm. Biopharm. 81 (2012) 294–302.
[41] C. Hassan, M.G. Kester, A.H. de Ru, P. Hombrink, J.W. Drijfhout, H. Nijveen, ... P.A. van Veelen, The human leukocyte antigen-presented ligandome of B lymphocytes, Mol. Cell. Proteom. 12 (2013) 1829–1843.
[42] E.M. Varypataki, K. van der Maaden, J. Bouwstra, F. Ossendorp, W. Jiskoot, Cationic liposomes loaded with a synthetic long peptide and poly(I:C): a defined adjuvanted vaccine for induction of antigen-specific T cell cytotoxicity, AAPS J. 17 (2015) 216–226.
[43] S. Mabrey, J.M. Sturtevant, Investigation of phase transitions of lipids and lipid mixtures by sensitivity differential scanning calorimetry, Proc. Natl. Acad. Sci. U. S. A. Vol. 73 (1976) 3862–3866.
[44] Y.P. Zhang, R.N. Lewis, R.N. McElhaney, Calorimetric and spectroscopic studies of the thermotropic phase behavior of the N-saturated 1,2-diacylphosphatidylglycerols, Biophys. J. 72 ((1997) 779–793.
[45] M. Gaestel, A. Herrmann, R. Heinrich, L. Pratsch, A.-M. Ladhoff, B. Hillebrecht, Lateral lipid distribution and phase transition in phosphatidylethanolamine/phosphatidylserine vesicles: a cross-linking study, Biochim. Biophys. Acta Biomembr. 732 (1983) 405–411.
[46] A.E. Regelin, S. Fankhaenel, L. Gurtesch, C. Prinz, G. von Kiedrowski, U. Massing, Biophysical and lipofection studies of dotap analogs, Biochim. Biophys. Acta 1464 (2000) 151–164.
[47] A.C.G. Weiss, K. Kempe, S. Forster, F. Caruso, microfluidic examination of the "hard" biomolecular corona formed on engineered particles in different biological milieu, Biomacromolecules 19 (11) (2018) 2580–2594.
[48] A. Mehlem, C.E. Hagberg, L. Muhl, U. Eriksson, A. Falkevall, Imaging of neutral lipids by oil red o for analyzing the metabolic status in health and disease, Nat. Protoc. 8 (2013) 1149.
[49] E. Kritikou, G.H. van Puijvelde, T. van der Heijden, P.J. van Santbrink, M. Swart, F.H. Schaftenaar, ... I. Bot, Inhibition of lysophosphatidic acid receptors 1 and 3 attenuates atherosclerosis development in Ldl-receptor deficient mice, Sci. Rep. 6 (2016) 37585.
[50] A. Wezel, M.R. de Vries, H.M. Lagraauw, A.C. Foks, J. Kuiper, P.H.A. Quax, I. Bot, Complement factor C5a induces atherosclerotic plaque disruptions, J. Cell. Mol. Med. 18 (2014) 2020–2030.
[51] S.K. Nadkarni, M.C. Pierce, B.H. Park, J.F. de Boer, P. Whittaker, B.E. Bouma, ... G.J. Tearney, Measurement of collagen and smooth muscle cell content in atherosclerotic plaques using polarization-sensitive optical coherence tomography, J. Am. Coll. Cardiol. 49 (2007) 1474–1481.
[52] M. Lundqvist, J. Stigler, G. Elia, I. Lynch, T. Cedervall, K.A. Dawson, Nanoparticle size and surface properties determine the protein corona with possible implications for biological impacts, Proc. Natl. Acad. Sci. U. S. A. 105 (2008) 14265–14270.
[53] N.S. Merle, S.E. Church, V. Fremeaux-Bacchi, L.T. Roumenina, Complement system part i - molecular mechanisms of activation and regulation, Front. Immunol. 6 (2015) 262.
[54] L.P. Erwig, P.M. Henson, Clearance of apoptotic cells by phagocytes, Cell Death Differ. 15 (2007) 243–250.
[55] D.A. Patten, S.K. Kamarajah, J.M. Rose, J. Tickle, E.L. Shepherd, D.H. Adams, ... S. Shetty, Scarf-1 promotes adhesion of Cd4(+) T cells to human hepatic sinusoidal endothelium under conditions of shear stress, Sci. Rep. 7 (2017) 17600.
[56] T. Iram, Z. Ramirez-Ortiz, M.H. Byrne, U.A. Coleman, N.D. Kingery, T.K. Means, ... J. El Khoury, Megf10 is a receptor for C1q that mediates clearance of apoptotic cells by astrocytes, J. Neurosci. 36 (2016) 5185–5192.
[57] G. Castellano, L.A. Trouw, N. Fiore, M.R. Daha, F.P. Schena, C. van Kooten, Infiltrating dendritic cells contribute to local synthesis of C1q in murine and human lupus nephritis, Mol. Immunol. 47 (2010) 2129–2137.
[58] A.C. Foks, D. Engelbertsen, F. Kuperwaser, N. Alberts-Grill, A. Gonen, J.L. Witztum, ... A.H. Lichtman, Blockade of Tim-1 and Tim-4 enhances atherosclerosis in low-density lipoprotein receptor-deficient mice, Arterioscler. Thromb. Vasc. Biol. 36 (2016) 456–465.
[59] M. van Oosten, E.S. van Amersfoort, T.J. van Berkel, J. Kuiper, Scavenger receptor-like receptors for the binding of lipopolysaccharide and lipoteichoic acid to liver endothelial and Kupffer cells, J. Endotoxin Res. 7 (2001) 381–384.
[60] K. Moore, F. Sheedy, E. Fisher, Macrophages in atherosclerosis: a dynamic balance, Nat. Rev. Immunol. 13 (2013) 709–721.
[61] A.C. Anselmo, M. Zhang, S. Kumar, D.R. Vogus, S. Menegatti, M.E. Helgeson, S. Mitragotri, Elasticity of nanoparticles influences their blood circulation, phagocytosis, endocytosis, and targeting, ACS Nano 9 (2015) 3169–3177.
[62] D. Christensen, M. Henriksen-Lacey, A.T. Kamath, T. Lindenstrøm, K.S. Korsholm, J.P. Christensen, ... E.M. Agger, A cationic vaccine adjuvant based on a saturated quaternary ammonium lipid have different in vivo distribution kinetics and display a distinct Cd4 T cell-inducing capacity compared to its unsaturated analog, J. Control. Release 160 (2012) 468–476.
[63] P. Gaitonde, A. Peng, R.M. Straubinger, R.B. Bankert, S.V. Balu-Iyer, Phosphatidylserine reduces immune response against human recombinant factor viii in hemophilia a mice by regulation of dendritic cell function, Clin. Immunol. 138 (2011) 135–145.
[64] C. Foged, C. Arigita, A. Sundblad, W. Jiskoot, G. Storm, S. Frokjaer, Interaction of dendritic cells with antigen-containing liposomes: effect of bilayer composition, Vaccine 22 (2004) 1903–1913.
[65] S. Ritz, S. Schottler, N. Kotman, G. Baier, A. Musyanovych, J. Kuharev, ... V. Mailander, Protein corona of nanoparticles: distinct proteins regulate the cellular uptake, Biomacromolecules 16 (2015) 1311–1321.
[66] D. Wang, B. Sun, M. Feng, H. Feng, W. Gong, Q. Liu, S. Ge, Role of scavenger receptors in dendritic cell function, Hum. Immunol. 76 (2015) 442–446.
[67] M. Miyanishi, K. Tada, M. Koike, Y. Uchiyama, T. Kitamura, S. Nagata, Identification of Tim4 as a phosphatidylserine receptor, Nature 450 (2007) 435–439.
[68] N. Kobayashi, P. Karisola, V. Pena-Cruz, D.M. Dorfman, M. Jinushi, S.E. Umetsu, ... G.J. Freeman, Tim-1 and Tim-4 glycoproteins bind phosphatidylserine and mediate uptake of apoptotic cells, Immunity 27 (2007) 927–940.
[69] M. He, H. Kubo, K. Morimoto, N. Fujino, T. Suzuki, T. Takahasi, ... H. Yamamoto, Receptor for advanced glycation end products binds to phosphatidylserine and assists in the clearance of apoptotic Cells, EMBO Rep. 12 (2011) 358–364.
[70] Z.G. Ramirez-Ortiz, W.F. Pendergraft 3rd, A. Prasad, M.H. Byrne, T. Iram, C.J. Blanchette, ... T.K. Means, The scavenger receptor Scarf1 mediates the clearance of apoptotic cells and prevents autoimmunity, Nat. Immunol. 14 (2013) 917–926.
[71] S.C. Choi, V.R. Simhadri, L. Tian, A. Gil-Krzewska, K. Krzewski, F. Borrego, J.E. Coligan, Cutting edge: Mouse Cd300f (Cmrf-35-like Molecule-1) recognizes outer membrane-exposed phosphatidylserine and can promote phagocytosis, J. Immunol. 187 (2011) 3483–3487.
[72] C. Bigler, M. Schaller, I. Perahud, M. Osthoff, M. Trendelenburg, Autoantibodies against complement C1q specifically target C1q bound on early apoptotic cells, J. Immunol. 183 (2009) 3512–3521.
[73] M. Son, B. Diamond, F. Santiago-Schwarz, Fundamental Role of C1q in autoimmunity and inflammation, Immunol. Res. 63 (2015) 101–106.
[74] D. Ugurlar, S.C. Howes, B.J. de Kreuk, R.I. Koning, R.N. de Jong, F.J. Beurskens, ... P. Gros, Structures of C1-Igg1 provide insights into how danger pattern recognition activates complement, Science 359 (2018) 794–797.
[75] K. von Kietzell, T. Pozzuto, R. Heilbronn, T. Grössl, H. Fechner, S. Weger, Antibody-mediated enhancement of parvovirus B19 uptake into endothelial cells mediated by a receptor for complement factor C1q, J. Virol. 88 (2014) 8102–8115.
[76] Z. Prohászka, J. Nemes, T. Hidvégi, F.D. Tóth, K. Kerekes, A. Erdei, ... G. Füst, Two parallel routes of the complement-mediated antibody-dependent enhancement of Hiv-1 infection, AIDS 11 (1997) 949–958.

[77] A. Takada, H. Feldmann, T.G. Ksiazek, Y. Kawaoka, Antibody-dependent enhancement of ebola virus infection, J. Virol. 77 (2003) 7539–7544.
[78] M.J. Walport, K.A. Davies, M. Botto, C1q and systemic lupus erythematosus, Immunobiology 199 (1998) 265–285.
[79] V.K. Bhatia, S. Yun, V. Leung, D.C. Grimsditch, G.M. Benson, M.B. Botto, ... D.O. Haskard, Complement C1q reduces early atherosclerosis in low-density lipoprotein receptor-deficient mice, Am. J. Pathol. 170 (2007) 416–426.
[80] A.J. Bradley, E. Maurer-Spurej, D.E. Brooks, D.V. Devine, Unusual electrostatic effects on binding of C1q to anionic liposomes: role of anionic phospholipid domains and their line tension, Biochemistry 38 (1999) 8112–8123.
[81] M.F. Bachmann, G.T. Jennings, Vaccine delivery: a matter of size, geometry, kinetics and molecular patterns, Nat. Rev. Immunol. 10 (2010) 787–796.
[82] A.J. Bradley, D.E. Brooks, R. Norris-Jones, D.V. Devine, C1q binding to liposomes is surface charge dependent and is inhibited by peptides consisting of residues 14-26 of the human C1qa chain in a sequence independent manner, Biochim. Biophys. Acta 1418 (1999) 19–30.
[83] K. Sou, E. Tsuchida, Electrostatic interactions and complement activation on the surface of phospholipid vesicle containing acidic lipids: effect of the structure of acidic groups, Biochim. Biophys. Acta 1778 (2008) 1035–1041.
[84] E.V. Clarke, B.M. Weist, C.M. Walsh, A.J. Tenner, Complement protein C1q bound to apoptotic cells suppresses human macrophage and dendritic cell-mediated Th17 and Th1 T cell subset proliferation, J. Leukoc. Biol. 97 (2015) 147–160.
[85] J.H.F. Stils, Adjuvants and antibody production: dispelling the myths associated with Freund's complete and other adjuvants, ILAR J. 46 (2005) 280–293.
[86] R. Klingenberg, N. Gerdes, R.M. Badeau, A. Gistera, D. Strodthoff, D.F. Ketelhuth, ... G.K. Hansson, Depletion of Foxp3+ regulatory T cells promotes hypercholesterolemia and atherosclerosis, J. Clin. Invest. 123 (2013) 1323–1334.
[87] A.C. Foks, V. Frodermann, M. ter Borg, K.L.L. Habets, I. Bot, Y. Zhao, ... G.H.M. van Puijvelde, Differential effects of regulatory t cells on the initiation and regression of atherosclerosis, Atherosclerosis 218 (2011) 53–60.
[88] X. Meng, W. Li, J. Yang, K. Zhang, W. Qin, G. An, ... Y. Zhang, T. Regulatory, Cells prevent plaque disruption in apolipoprotein E-knockout mice, Int. J. Cardiol. 168 (2013) 2684–2692.